Regulation of pri-miRNA processing by the hnRNP-like protein *At*GRP7 in Arabidopsis

Tino Köster[1], Katja Meyer[1], Claus Weinholdt[2], Lisa M. Smith[3,4], Martina Lummer[1], Corinna Speth[3,5,6], Ivo Grosse[2,7], Detlef Weigel[3] and Dorothee Staiger[1,8,*]

[1]Molecular Cell Physiology, Bielefeld University, [2]Institute of Computer Science, Martin-Luther-University Halle-Wittenberg, Germany, [3]Max Planck Institute for Developmental Biology, Tuebingen, Germany, [4]Department of Animal & Plant Sciences, University of Sheffield, UK, [5]Center for Plant Molecular Biology, University of Tuebingen, [6]Chemical Genomics Centre of the Max Planck Society, Dortmund, Germany, [7]German Centre for Integrative Biodiversity Research Halle-Jena-Leipzig, Germany and [8]Institute for Genome Research & Systems Biology, CeBiTec, Bielefeld, Germany

ABSTRACT

The hnRNP-like glycine-rich RNA-binding protein *At*GRP7 regulates pre-mRNA splicing in Arabidopsis. Here we used small RNA-seq to show that *At*GRP7 also affects the miRNA inventory. *At*GRP7 overexpression caused a significant reduction in the level of 30 miRNAs and an increase for 14 miRNAs with a minimum log$_2$ fold change of ±0.5. Overaccumulation of several pri-miRNAs including pri-miR398b, pri-miR398c, pri-miR172b, pri-miR159a and pri-miR390 at the expense of the mature miRNAs suggested that *At*GRP7 affects pri-miRNA processing. Indeed, RNA immunoprecipitation revealed that *At*GRP7 interacts with these pri-miRNAs *in vivo*. Mutation of an arginine in the RNA recognition motif abrogated *in vivo* binding and the effect on miRNA and pri-miRNA levels, indicating that *At*GRP7 inhibits processing of these pri-miRNAs by direct binding. In contrast, pri-miRNAs of selected miRNAs that were elevated or not changed in response to high *At*GRP7 levels were not bound *in vivo*. Reduced accumulation of miR390, an initiator of *trans*-acting small interfering RNA (ta-siRNA) formation, also led to lower *TAS3* ta-siRNA levels and increased mRNA expression of the target *AUXIN RESPONSE FACTOR4*. Furthermore, *At*GRP7 affected splicing of pri-miR172b and pri-miR162a. Thus, *At*GRP7 is an hnRNP-like protein with a role in processing of pri-miRNAs in addition to its role in pre-mRNA splicing.

INTRODUCTION

Post-transcriptional regulation makes an important contribution to co-ordinating eukaryotic gene expression programs. This control at the RNA level can be executed by proteins or small RNAs. RNA-binding proteins (RBPs) specifically interact with defined sequence motifs in mRNAs to control pre-mRNA splicing, nuclear export or RNA decay (1–3). An abundant class of RBPs comprises the heterogeneous nuclear ribonucleoproteins (hnRNPs), originally identified on the basis of their association with nascent pre-mRNAs (4). More recently, hnRNPs have been shown to mediate many steps in RNA maturation (5,6). Among small regulatory RNAs are the microRNAs (miRNAs) that interact with complementary sites in mRNAs to determine their availability for translation. MiRNAs and their targets are collectively referred to as miRNA modules (7). MiRNAs are 21–24 nt-long single-stranded RNAs generated from precursors that are transcribed by RNA polymerase II (8–10). In Arabidopsis, these pri (primary)-miRNAs are stabilized by DAWDLE (DDL), a forkhead-associated domain protein that likely recruits processing factors (11). The pri-miRNAs contain imperfect double-stranded fold-back structures and endonucleolytic cleavage by the RNaseIII family protein DICER-LIKE1 (DCL1) first releases the stem–loops, giving rise to pre (precursor)-miRNAs. These are further processed by DCL1 into duplexes of the miRNA guide strand and the miRNA* passenger strand. The miRNA/miRNA* duplexes have 2-nt overhangs at the 3′end that are methylated at the 2′-OH groups by HUA ENHANCER 1 (12), and poly(U) tails are added. These features prevent degradation of the miRNAs (12,13).

After export to the cytoplasm the miRNA/miRNA* duplexes dissociate and the miRNA guide strand binds to ARGONAUTE1 (AGO1) or other members of the AGO family. The resulting RNA-induced silencing complexes

*To whom correspondence should be addressed. Tel: +49 521 106 5609; Fax: +49 521 106 6410; Email: dorothee.staiger@uni-bielefeld.de

guide the AGO proteins to complementary sites in the miRNA targets, leading to their down-regulation by AGO cleavage or inhibition of translation (14,15). Although the miRNA* strand initially was thought to simply decay, accumulating evidence points to a functional role for some miRNA*s (16,17).

The double-stranded RBP HYPONASTIC LEAVES1 (HYL1), the zinc finger protein SERRATE (SE) and the G-patch domain protein TOUGH (TGH) contribute to pri-miRNA processing (18). Together with DCL1, these proteins form the so-called Microprocessor complex that is tethered to the pri-miRNA via interaction with the cap binding proteins CBP20 and CBP80 (19–21). SE and HYL1 promote accurate pri-miRNA processing by DCL1 (22,23), and TGH enhances DCL1 activity without influencing the processing accuracy (18). Thus, several classes of RBPs are involved in miRNA processing. As such a function has not yet been described for a plant hnRNP protein, we investigated whether the glycine-rich hnRNP-like protein *At*GRP7 (*Arabidopsis thaliana* glycine-rich RBP 7) has an effect on miRNA metabolism. *At*GRP7 consists of an RNA recognition motif (RRM) and a namesake glycine stretch. It responds to abiotic stress, is controlled by the circadian clock and participates in pathogen defense (24–29). *At*GRP7 was the first hnRNP-like protein in plants that was shown to regulate alternative splicing by direct binding to pre-mRNAs (30).

Here we used small RNA sequencing to show that *At*GRP7 affects the miRNA inventory. We identified 44 miRNAs with altered levels in plants ectopically expressing *At*GRP7 (*At*GRP7-ox). An increased level of several primary transcripts was found at the expense of the mature miRNAs. Furthermore, *At*GRP7 interacted with these pri-miRNAs *in vivo* and this interaction was lost upon mutation of a single conserved arginine residue in the RRM. Moreover, *At*GRP7 affected alternative splicing of pri-miR172b and pri-miR162a. Thus, we identify a novel function for a plant hnRNP-like RBP in pri-miRNA processing.

MATERIALS AND METHODS

Transgenic plants

*At*GRP7-ox and *At*GRP7-R^{49}Q-ox plants express the *At*GRP7 wild-type (wt) coding sequence or a mutant version with Arg49 exchanged for Gln under control of the Cauliflower Mosaic Virus (CaMV) 35S promoter in the C24, Col-2 and Landsberg *erecta* accessions (31–34). *At*GRP8-ox plants express the *At*GRP8 coding region under control of the CaMV promoter in Col-2 (30). The line *AtGRP7::AtGRP7:GFP* expresses an *At*GRP7 green fluorescent protein (GFP) fusion under control of 1.4 kb of the *AtGRP7* promoter and the *AtGRP7* 5'UTR, intron and 3'UTR in *atgrp7–1*, and the line *AtGRP7::GFP* expresses GFP only under control of the *AtGRP7* promoter, 5'UTR and 3'UTR (30,35). To generate an *AtGRP7::AtGRP7-R^{49}Q:GFP* fusion protein, the 529 bp SacI-XmnI fragment in the *AtGRP7::AtGRP7:GFP* construct was exchanged with the corresponding fragment carrying the R^{49}Q mutation and the construct was introduced into the *atgrp7–1* background. The *AtGRP8::AtGRP8:GFP* construct includes 1.9 kb of the *AtGRP8* promoter and the native

5'UTR, 3'UTR and intron and was introduced into Col-2. The *atgrp7–1* mutant lacks detectable *At*GRP7 expression due to a T-DNA insertion in the 5'UTR but has elevated levels of the paralog *At*GRP8 due to relief from repression by *At*GRP7, and the *atgrp7–1 8i* mutant lacks *At*GRP7 and has wt levels of *At*GRP8 due to an *AtGRP8* RNAi construct (30,36).

Plant growth

Arabidopsis seeds were surface-sterilized and sown on half-strength MS (Murashige–Skoog) (Duchefa) plates (37). Plants were grown in light/dark cycles at 20°C in Percival incubators (CLF laboratories). For RNA analysis, aerial parts of the plants were harvested. At least 10 plants were bulked for each sample in each replicate.

RNA analysis

For RNA analysis, about ten 14-day-old plants per time point were pooled and RNA was isolated using TRIzol® reagent (Invitrogen). For small RNA gel blots, 30 µg of total RNA was fractionated on a 17% polyacrylamid–8 M urea gel in 3-(*N*-morpholino)propanesulfonic acid buffer, transferred onto GeneScreen membrane and cross-linked with 1-ethyl-3,2-dimethylcarbodiimide and 1-methylimidazole (38). Hybridisation was performed with radiolabeled antisense oligonucleotides in PerfectHybPlus buffer (Sigma) at 38°C. Blots were analysed using a Typhoon 8000 PhosphorImager and ImageQuant software (Amersham Pharmacia Biotech, http://www5.amershambiosciences.com/). Quantification of real-time PCR (RT-PCR) products was done using DNA1000 chips on an Agilent 2100 bioanalyzer. RT-PCR and quantification of miRNAs by stem–loop RT-PCR were done as described (39,40). Primers are listed in Supplementary Table S1.

RNA immunoprecipitation

Plants expressing *At*GRP7, *At*GRP8 or *At*GRP7-R^{49}Q fused to GFP or GFP only were subjected to RNA immunoprecipitation (RIP) as previously described (41). Briefly, plants were subjected to formaldehyde fixation and the extract was subjected to IP with GFP-Trap® beads (Chromotek) (IP+) and mock IP with RFP-Trap® beads (Chromotek) (IP−). Coprecipitated RNAs were identified via RT-PCR. In parallel, transcript levels were determined in RNA isolated from the extract before addition of the beads (input).

Small RNA libraries and sequencing

*At*GRP7-ox and Col-2 plants were grown for 23 days on half-strength MS medium containing 1% sucrose. Total RNA was extracted from aerial tissue using TRIzol® reagent (Invitrogen). Small RNA libraries were prepared from two biological replicates using the NEB Next® Small RNA Sample Prep Set 1 kit (NEB). Before and after adapter ligation, RNA was size-fractionated on urea-PAGE gels. PCR amplification was done with Phusion® polymerase (Finnzymes) and primers supplied in the NEBNext® Small

RNA Sample Prep Set 1 kit. The quality of the library was checked on a DNA1000 Bioanalyzer chip and sequencing was performed on the HiSeq2000 Illumina system with a read length of 50 nt.

Bioinformatic evaluation of small RNA-seq data

Reads were mapped onto the Arabidopsis genome (TAIR10) using Bowtie (v0.12.9) without allowing mismatches (42). Mapped reads were counted using the Bedtools (v2.17.0) script coverageBed (43) with the annotation file from miRBase (http://www.mirbase.org/). For mature miRNAs we counted only reads that matched perfectly to the miRBase annotated region without any shift. The differential expression analysis was performed with Bioconductor (2.13) package DESeq (44). MiRNAs were declared as differentially expressed if the adjusted *P*-value (*p*adj) was below 0.1. To determine miRNAs differentially expressed in the *tough* mutant (18) the read counts of the dataset (GSE38600) were used.

Processing accuracy of small RNAs

To assess the accuracy of pri-miRNA processing the mapping positions were combined with the annotations for miRNAs from miRBase. The annotated start site at the 5′end and end site at the 3′end were denoted by ASS and AES, and the mapped start and end sites were denoted by MSS and MES, respectively. For each miRNA the distance $D_{start} = $ ASS–MSS and the distance $D_{end} = $ AES–MES was calculated. The histograms of D_{start} and D_{end} were calculated separately for Col-2 and *At*GRP7-ox.

Immunoblot analysis

Total protein was isolated as described (45). Chemiluminescence detection of the immunoblots was done with Stella (Raytest) and signals were quantified using the AIDA software. The antibodies are listed in Supplementary Table S2.

Confocal microscopy

Transient expression in *Nicotiana benthamiana* leaves was performed as described (46) and analyzed using a LSM 780 confocal laser scanning microscope (Zeiss). Constructs are described in Supplementary Table S3.

RESULTS

MiR398 abundance is reduced in *At*GRP7-ox plants

Genome-wide transcriptome analysis of *At*GRP7-ox plants had previously revealed an elevated steady-state abundance of the *COPPER ZINC SUPEROXIDE DISMUTASE 2* (*CSD2*) transcript encoding a superoxide dismutase that uses copper as a metal cofactor (47). CSD2 is a target of the miR398 family, which comprises identical miRNAs encoded by *MIR398b* and *MIR398c* on chromosome V, and a miRNA with a 3′ U instead of G encoded by *MIR398a* on chromosome II (48,49). To test whether the altered *CSD2* transcript level in *At*GRP7-ox plants reflected an impact
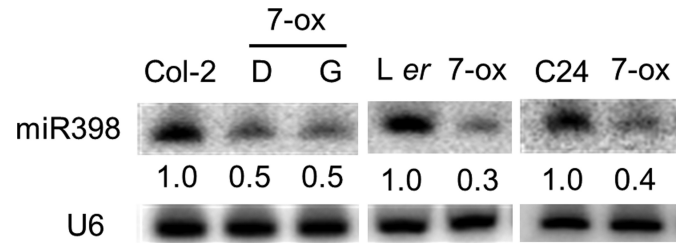

Figure 1. MiR398 levels are reduced in *At*GRP7-ox plants. An RNA gel blot of the *At*GRP7-ox lines D and G in Col-2, *At*GRP7-ox lines in L *er* and C24 and the corresponding wt plants was hybridised with anti-miR398 (top) and a U6 control (bottom). Fold changes of miR398 normalized to U6 in *At*GRP7-ox plants are expressed relative to wt.

of *At*GRP7 on miR398, we monitored miR398 levels using low molecular weight northern blot analysis. MiR398 steady-state abundance was reduced in *At*GRP7-ox lines in the Col-2, L *er* and C24 accessions compared to the corresponding wt plants (Figure 1).

Small RNA profiling reveals a widespread impact of *At*GRP7 on the miRNome

To test whether *At*GRP7 affects miRNA levels more globally, small RNA libraries were constructed from *At*GRP7-ox and wt plants for high-throughput sequencing. Among 223 miRNAs mapping to the genome with a perfect match, 53 were excluded from further analysis because they were represented by fewer than five reads. The levels of 118 of the remaining 170 miRNAs were not significantly altered. Thus, *At*GRP7 overexpression does not have a general effect on miRNA abundance (Supplementary Figure S1A). We tested the validity of our analyses by examining in the same manner a published dataset for the mutant defective in TOUGH (18); our pipeline confirmed a widespread alteration in miRNA abundance in *tgh* (Supplementary Figure S1B). Of the 52 miRNAs that were significantly changed relative to wt in the *At*GRP7-ox plants in two biological replicates, 30 miRNAs showed a log$_2$ fold change < -0.5 and the level of 14 miRNAs showed a log$_2$ fold change >0.5 (Supplementary Figure S2, Supplementary Tables S4 and S5). Most of the miRNAs with elevated levels showed only a low read coverage and therefore we mainly focussed on miRNAs with reduced levels upon *At*GRP7 overexpression.

Reduced miR398 levels correlate with elevated levels of CSD and CCS in *At*GRP7-ox but not *At*GRP7-R^{49}Q-ox plants

To validate the RNA-seq data, steady-state abundance of selected miRNAs was monitored by stem–loop RT-PCR. In independent *At*GRP7-ox lines grown on half-strength MS medium, miR398 levels reached only 25–50% of the wt level (Figure 2A, Supplementary Figure S3). In contrast, in plants overexpressing *At*GRP7 with a single arginine in the RRM mutated (*At*GRP7-R^{49}Q-ox) (32) miR398 levels were similar to wt levels. This suggests that *At*GRP7 contributes to reduced miR398 steady-state abundance through a mechanism requiring RNA binding. Transcript levels of the miR398 targets CSD1 localized in the cytosol, CSD2 localized in the chloroplast and CCS (COPPER CHAPERONE
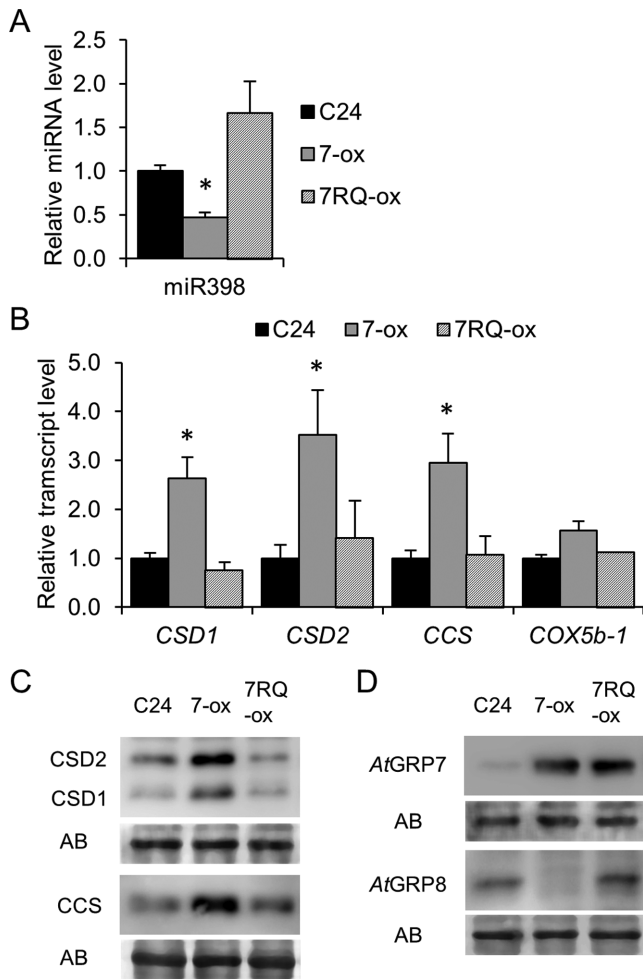
Figure 2. MiR398 and miR398 targets are affected in *At*GRP7-ox but not *At*GRP7-R^{49}Q-ox plants. (**A**) Stem–loop RT-PCR of miR398. Shown are the mean ± SD of three biological replicates. Asterisks denote statistically significant differences according to Student's t-test ($P < 0.05$). (**B**) Relative transcript levels of the miR398 targets *CSD1*, *CSD2*, *CCS* and *COX5b-1*. (**C**) CSD1, CSD2 and CCS protein levels. AB, Amidoblack staining of the membrane to show equal loading. (**D**) *At*GRP7 and *At*GRP8 protein levels.

FOR CSD) that delivers the copper cofactor to the CSDs (50) were elevated in *At*GRP7-ox but not *At*GRP7-R^{49}Q-ox plants (Figure 2B). The abundance of the predicted target *COX5b-1* was not altered in *At*GRP7-ox plants, in agreement with a previous observation that *COX5b-1* is not substantially regulated by miR398 (51). An immunoblot analysis demonstrated elevated levels of CSD2, CSD1 and CCS in *At*GRP7-ox but not *At*GRP7-R^{49}Q-ox plants (Figure 2C). Taken together, the reduced miR398 level in *At*GRP7-ox plants correlates with elevated *CSD1*, *CSD2* and *CCS* transcript and protein levels.

To determine whether the altered CSD and CCS levels in *At*GRP7-ox plants indeed depend on miR398, we used the observation that an exposure of plants to a high Cu^{2+} concentration that provokes oxidative stress shuts down *MIR398* promoter activity with subsequent accumulation of *CSD2* mRNA (52,53). The half-strength MS medium used in all experiments contains 0.05 μM Cu^{2+} allowing the *MIR398b and c* promoters to be active (54). When the medium was supplemented with 15 μM Cu^{2+} that inhibits *MIR398b* and *c* promoter activity (52,53), no miR398 was detected and CSD1, CSD2 and CCS accumulated to the same high level in both wt and *At*GRP7-ox plants (Supplementary Figure S4). Thus, in the absence of miR398, elevated *At*GRP7 levels do not provoke a further increase beyond wt.

*At*GRP7 affects miR390-dependent *TAS3* ta-siRNAs

*At*GRP7-ox plants have reduced levels of miR390, the initiator of *TAS3* ta-siRNA biogenesis (Figure 3A). This indicates that *At*GRP7 also affects miRNAs that are loaded into AGO2 and AGO7 (16,55). We investigated whether the miR390-dependent *TAS3* ta-siRNAs are likewise affected. A lower read coverage was observed for all three *TAS3* loci in *At*GRP7-ox plants (Supplementary Figure S5). Stem–loop RT-PCR confirmed that *TAS3 5′D7(+)* levels were reduced in *At*GRP7-ox but not *At*GRP7-R^{49}Q-ox plants (Figure 3B, Supplementary Figure S6). Furthermore, expression of the ta-siRNA target *ARF4* was elevated in *At*GRP7-ox but not *At*GRP7-R^{49}Q-ox plants (Figure 3C).

We also confirmed that the levels of both miR172 and miR172b* were significantly reduced in *At*GRP7-ox plants (Supplementary Figure S7A). MiR172 targets *APETALA-2* type transcription factors mostly at the translational level although slicing also occurs (56,57). Levels of *SCHLAF-MUETZE* (*SMZ*), a miR172 target regulated by slicing (57), were elevated in *At*GRP7-ox plants (Supplementary Figure S7B). Of the miR167 family, miR167c was significantly reduced (Supplementary Table S4) and miR167a and b were weakly reduced in *At*GRP7-ox plants. This was confirmed by stem–loop RT-PCR, and the level of its target *AUXIN RESPONSE FACTOR8* (*ARF8*) (58) was increased. For miR824, a recently evolved miRNA encoded by a single locus (59,60) that was expressed at reduced levels in *At*GRP7-ox plants, the level of its target *AGL16* that has been implicated in stomatal density (61) was slightly elevated in the *At*GRP7-ox lines.

For miR159, RNA-seq had not revealed any difference in the miR159a, b and c isoforms in *At*GRP7-ox plants whereas stem–loop RT-PCR revealed a reduced level of miR159. The levels of its targets, the MYB33 and MYB65 transcription factors that control many processes including leaf development and flowering time (62) were increased in *At*GRP7-ox plants, suggesting that in this case stem–loop RT-PCR may more faithfully reflect the *in vivo* situation. Such discrepancies in comparing miRNA levels by RNA-seq or RT-PCR based methods have been previously discussed (63).

Among miRNAs with elevated levels in *At*GRP7-ox plants compared to wt were members of the miR395 family that is involved in the response to sulfate starvation (Supplementary Figure S7A). The target ATP sulfurylase 3 (APS3), one of the isoenzymes catalyzing the first step of sulfate assimilation, was present at reduced levels in *At*GRP7-ox plants (Supplementary Figure S7B). Taken together, altered miRNA levels were confirmed in independent *At*GRP7-ox plants and correlated with altered target levels for a suite of the miRNA modules.
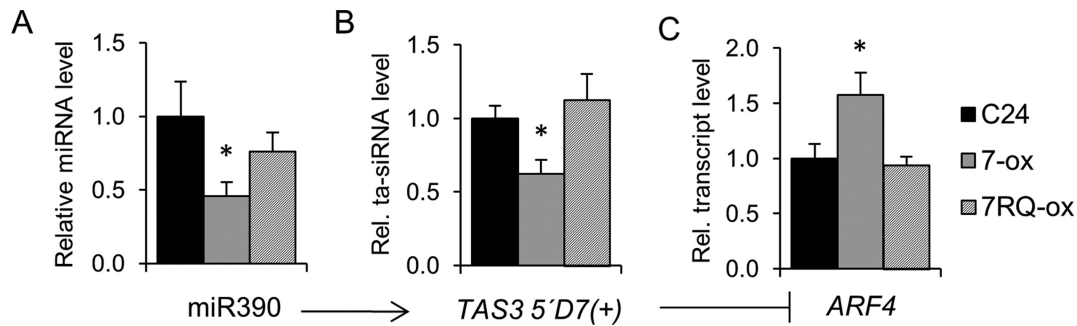
Figure 3. *At*GRP7 affects miR390-dependent *TAS3* ta-siRNAs and *ARF4* in *At*GRP7-ox but not *At*GRP7 R^{49}Q-ox plants. (**A**) Stem–loop RT-PCR of miR390. (**B**) Stem–loop RT-PCR of *TAS3 5′D7(+)* RNA. (**C**) Levels of the miR390 target *ARF4*. Shown are the mean ± SD of three biological reps. Asterisks denote statistically significant differences according to Student's t-test ($P < 0.05$).

Levels of several pri-miRNAs are inversely correlated with mature miRNAs in *At*GRP7-ox plants

The altered steady-state level of miRNAs in *At*GRP7-ox plants could be a consequence of altered levels of pri-miRNAs or altered fates of mature miRNAs. RT-PCR analysis revealed significantly elevated levels of pri-miR398a, pri-miR398b and pri-miR398c in *At*GRP7-ox but not *At*GRP7-R^{49}Q-ox plants (Figure 4A and B). Similarly, the primary transcript for miR390b that initiates *TAS3* cleavage in ta-siRNA generation was significantly elevated in *At*GRP7-ox but not *At*GRP7-R^{49}Q-ox plants. Furthermore, we found elevated levels of pri-miR172b and pri-miR159a in independent *At*GRP7-ox lines (Figure 4B). As the miR159 precursor is processed by an unusual mechanism with the initial cut near the loop of the stem rather than at its base (64), *At*GRP7 appears to affect miRNA precursors processed by the conventional base-to-loop mechanism and precursors processed in loop-to-base direction (Supplementary Tables S4 and S5). The elevated pri-miR399b levels (Figure 4B) correlate with the reduced miR399b level found by RNA-seq.

The miR395 and miR319 families are examples of miRNAs with elevated levels in *At*GRP7-ox plants. Pri-miR395e levels were slightly but not significantly reduced and pri-miR319b levels were not altered in *At*GRP7-ox plants (Figure 4C), suggesting that *At*GRP7 affects different pri-miRNAs by different means. We also monitored the precursors of miR408 and miR171 that were not affected by *At*GRP7 and found pri-miR408a and pri-miR171c at similar levels in wt and independent *At*GRP7-ox lines.

*At*GRP7 does not affect levels of pri-miRNA processing components

The accumulation of pri-miRNAs at the expense of mature miRNAs in *At*GRP7-ox plants indicates that *At*GRP7 contributes to pri-miRNA processing. To determine whether this is an indirect effect caused by misexpression of general processing factors, we monitored levels of pri-miRNA processing components and additional factors that affect miRNA levels in Arabidopsis. The steady-state abundance of the *CBP80*, *HYL1*, *DCL1*, *SE*, *DDL*, *HEN1* and *TGH* transcripts was not consistently altered (Supplementary Figure S8A and B). This was also the case for mRNAs encoding MOS2 (MODIFIER OF SCN1, 2) that facili-
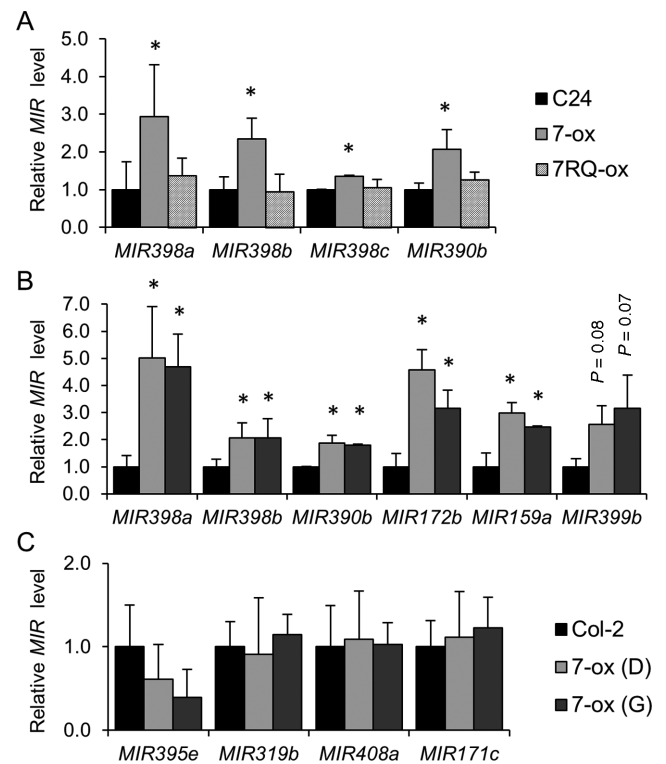

Figure 4. Pri-miRNA levels are elevated at the expense of mature miR-NAs in *At*GRP7-ox plants. The levels of the pri-miRNAs were analyzed in *At*GRP7-ox, *At*GRP7-R^{49}Q-ox and C24 wt plants (**A**) and in the *At*GRP7-ox lines D and G and Col-2 (**B, C**). Pri-miR398a, b and c, pri-miR390b, pri-miR172b, pri-miR159a and pri-miR399b correspond to miRNAs with reduced level in *At*GRP7-ox plants. Pri-miR395e and pri-miR319b correspond to miRNAs with elevated levels in *At*GRP7-ox plants, and pri-miR408a and pri-miR171c correspond to miRNAs that are not affected by *At*GRP7 overexpression. Data are based on three biological reps. Asterisks denote a significant difference according to Student's t-test ($P < 0.05$).

tates recruitment of pri-miRNAs to the Dicing complex (65), and the proline-rich protein SICKLE (SIC) which is required for accumulation of a subset of miRNAs (66). *CBP20* was expressed at a higher level upon *At*GRP7 overexpression in C24 but not in Col-2, and the CBP20 protein level was not elevated. The transcript encoding CDC5 (CELL DIVISION CYCLE 5) that functions as an activa-

tor of pri-miRNA transcription and promotes processing of several pri-miRNAs (67) was not significantly affected by *At*GRP7. Similarly, the transcripts of the RACK1A (RECEPTOR FOR ACTIVATED C KINASE 1A), RACK1B and RACK1C proteins that interact with SE and act redundantly on miRNA accumulation (40) were not affected. Furthermore, levels of HYL1, CBP80 and SE protein were not altered in *At*GRP7-ox plants (Supplementary Figure S8C and D). Thus, *At*GRP7 does not have a significant impact on miRNA processing factors.

*At*GRP7 binds pri-miRNAs *in vivo*

Because *At*GRP7 did not appear to affect miRNA levels indirectly via a global effect on processing factors, we tested whether it directly interacts with pri-miRNAs *in vivo*. We performed RIP on transgenic plants expressing *At*GRP7:GFP under control of its own promoter in the *atgrp7–1* background. Pri-miR398b and pri-miR398c were enriched in RNP complexes precipitated with GFP-Trap® beads (IP+) from these *AtGRP7::AtGRP7:GFP* plants relative to mock precipitates with RFP-Trap® beads (IP−) (Figure 5A). *PP2A* which served as a negative control was not significantly enriched. Both pri-miR398b and pri-miR398c were not enriched in precipitates from plants expressing GFP alone. Notably, they were also not recovered from plants expressing *AtGRP7::AtGRP7-R⁴⁹Q:GFP* (Figure 5B). The pri-miR398a level was too low to allow reliable quantification, in line with its weak expression (68). Furthermore, pri-miR172b and pri-miR159a were enriched in IP+ relative to IP− and not present in precipitates from plants expressing *AtGRP7::AtGRP7-R⁴⁹Q:GFP* or GFP only. For pri-miR390b, the expression level was also too low to allow reliable quantification.

If direct binding of *At*GRP7 to the pri-miRNA has a functional consequence, the primary transcripts of miRNAs with unaltered levels should not be targets. Indeed, no enrichment of pri-miR408a, pri-miR171b and pri-miR171c in RIP of *AtGRP7::AtGRP7:GFP* plants was detected (Figure 5D). Similarly, pri-miR319b was not enriched. miR319 is an example of a miRNA with an elevated level in *At*GRP7-ox plants but pri-miRNA level is not altered. This suggests that the effect of *At*GRP7 on miR319 is indirect.

*At*GRP7 colocalizes with processing components

Binding of *At*GRP7 to pri-miRNAs *in vivo* implies a direct role in processing. Therefore, we compared the subcellular localization of *At*GRP7 to that of other processing components by transient coexpression of fluorescent protein-tagged fusion proteins in *N. benthamiana* leaves (Supplementary Figure S9). *At*GRP7 colocalizes with DCL1, SE, DDL and CBP80 in the nucleus. In the case of DCL1 and SE the colocalization is confined to the nucleoplasm whereas DDL and CBP80 also localize to the nucleolus, as does *At*GRP7. For DCL1, we detected colocalization in punctate structures in the nucleus, likely representing dicing bodies that are known sites of miRNA processing (69–71).

The paralogous *At*GRP8 can compensate for loss of *At*GRP7

As elevated levels of *At*GRP7 impair processing of a suite of pri-miRNAs, we asked whether the absence of *At*GRP7 would likewise have an effect. Levels of mature miR398 were not significantly changed in the *atgrp7–1* line that lacks *At*GRP7 but has higher levels of its paralog *At*GRP8 than wt due to relief from repression by *At*GRP7 (Supplementary Figure S10A and B). It was also not changed in the line *atgrp7–1 8i* that lacks *At*GRP7 and has wt levels of *At*GRP8 due to an RNAi construct. Pri-miR398a and pri-miR398b levels were slightly but significantly decreased in *atgrp7–1 8i* and thus changed in the opposite direction in response to elevated and reduced *At*GRP7, respectively, as expected for a direct target (Supplementary Figure S10C). The level of pri-miR398c was not consistently altered either in *atgrp7–1* or *atgrp7–1 8i*. Similarly, levels of miR172b*, miR395 and miR159 were not altered. Neither were the levels of miR390, the *TAS3 5′D7(+)* ta-siRNA and *ARF4* altered (Supplementary Figure S10D–F). Thus, while *At*GRP7 clearly contributes to processing of a subset of pri-miRNAs, a reduced level appears to be compensated by other factors.

To test whether the residual *At*GRP8 in the *atgrp7 8i* line may mask the loss of *At*GRP7, we tested the effect of *At*GRP8 on miRNA levels. In the absence of a true *atgrp8* loss-of-function mutant, we investigated *At*GRP8-ox plants and found the levels of miR398 to be reduced to ∼35% of the wt level and miR172 and miR159 to be reduced to ∼50% (Supplementary Figure S11A). In turn, the levels of pri-miR398b, pri-miR172b and pri-miR159a were elevated (Supplementary Figure S11B). This suggests that *At*GRP8 in addition to *At*GRP7 promotes the accumulation of these pri-miRNAs at the expense of the mature miRNA and thus the presence of *At*GRP8 in *atgrp7–1* or *atgrp7–1 8i* masks the mutant phenotype.

To test whether *At*GRP8 is also able to interact *in vivo* with the pri-miRNAs it regulates, we generated transgenic plants expressing *AtGRP8::AtGRP8:GFP*. Pri-miR398b, pri-miR398c, pri-miR172b and pri-miR159a indeed also coprecipitated with *At*GRP8 (Supplementary Figure S11C). The weaker enrichment compared to the *At*GRP7 RIP likely is due to competition by the endogenous *At*GRP8 and *At*GRP7 proteins, as in the absence of a true *atgrp8* loss-of-function mutant, the *AtGRP8::AtGRP8:GFP* line had to be generated in the wt background. As a control, we monitored the interaction of *At*GRP8:GFP with *AtGRP7* and *AtGRP8* itself that had been demonstrated *in vitro* (28). We confirmed that *At*GRP8 interacts with these transcripts also *in vivo*.

Processing accuracy in *At*GRP7-ox and wt plants

Altered levels of miRNAs in *At*GRP7-ox plants may be due to imprecise processing of pri-miRNAs such that the excised miRNAs would not fall exactly within the annotated mature miRNA positions. Therefore, the start positions at the 5'end and the end positions at the 3'end of each excised miRNA in wt and *At*GRP7-ox plants were compared to the start and end positions annotated in miRBase. The resulting differences of the mapped and annotated start sites or end sites are presented in Supplementary Figure S12. The distribution showed a strong peak at the annotated 5′ and
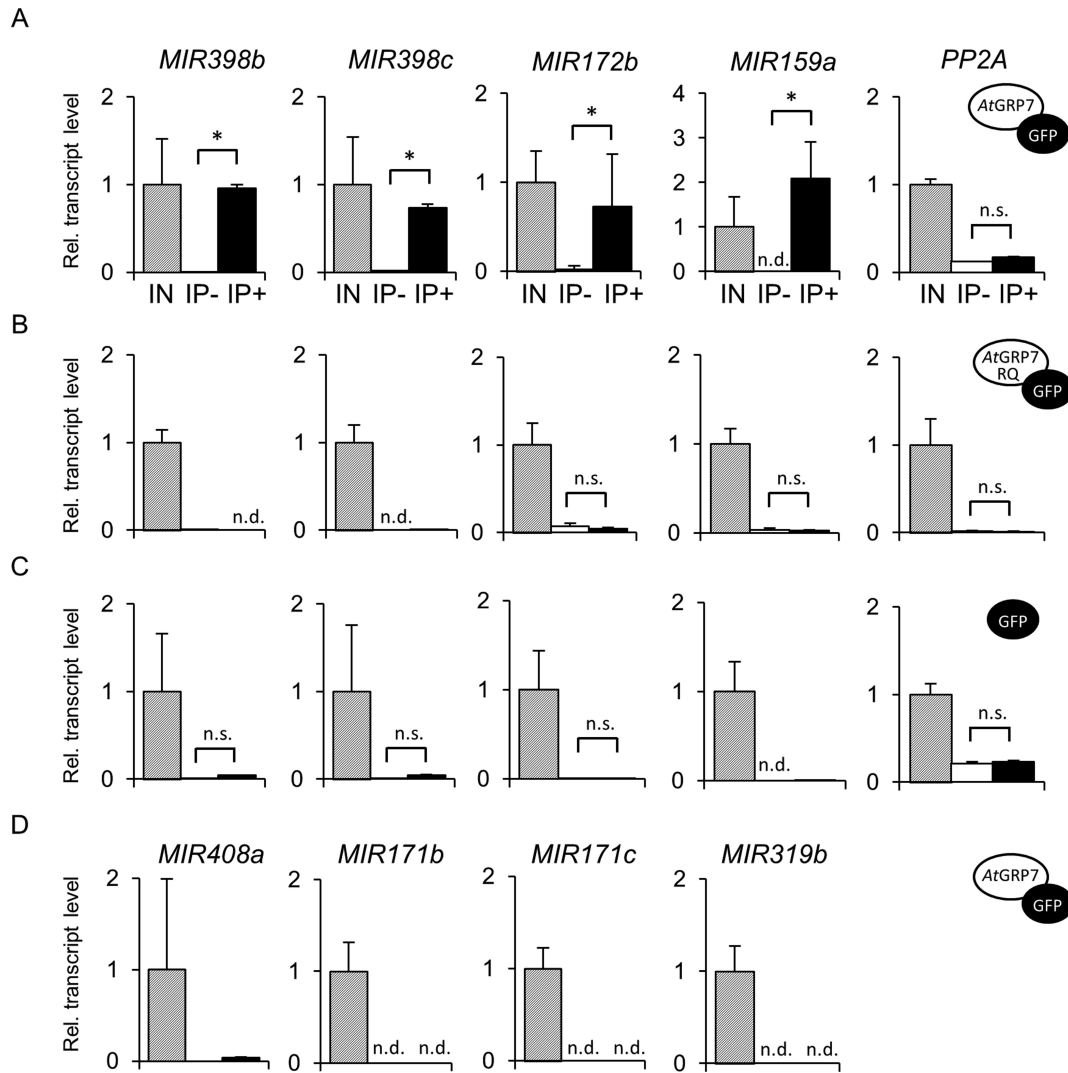
Figure 5. *At*GRP7 binds to pri-miRNAs *in vivo*. Plants expressing *AtGRP7::AtGRP7:GFP* (**A, D**) or *AtGRP7::AtGRP7-R^{49}Q:GFP* (**B**) in the *atgrp7–1* background and *AtGRP7:GFP* in Col-2 (**C**) were subjected to RIP. The levels of the pri-miRNAs and *PP2A* were determined in the GFP-Trap® bead precipitate (IP+), the RFP-Trap® bead precipitate (IP−) and the input fraction (IN), respectively. Pri-miR398b and c, pri-miR172b and pri-miR159a correspond to miRNAs with reduced level in *At*GRP7-ox plants, pri-miR319b corresponds to a miRNA with elevated levels in *At*GRP7-ox plants, and pri-miR408a and pri-miR171 b and c correspond to miRNAs that are not affected. Data are based on three biological replicates. Asterisks denote a significant difference according to Student's t-test ($P < 0.05$). n.s., not significant; n.d., not detectable.

3′ends both in wt and *At*GRP7-ox, suggesting that *At*GRP7 does not generally affect processing accuracy.

Furthermore, we mapped all reads to the annotated pri-miRNAs and found no major products from non-standard processing outside the annotated miRNA and miRNA* positions (Supplementary Figure S13). Finally, to test whether miRNAs of unusual size accumulate in *At*GRP7-ox plants, the read length distributions of the excised miRNAs were compared between wt and *At*GRP7-ox plants. Most pri-miRNAs in *At*GRP7-ox plants released sRNAs with a similar size distribution to that in wt (Supplementary Figure S14). Taken together, this suggests that *At*GRP7 does not generally affect processing accuracy.

Whereas in animals miRNA precursors have a fold-back structure of similar size, plant miRNA precursors can adopt a wide range of structures and the fold-back structures can be up to 900 nt in length (72). To investigate whether the

action of *At*GRP7 on a miRNA may correlate with the length of its fold-back structure, we retrieved the sizes of 329 miRNA stem–loops from miRBase. The size distribution of precursors of the miRNAs with significantly reduced or elevated levels in *At*GRP7-ox plants did not deviate from the overall size distribution (Supplementary Figure S15). Thus, the length of the fold-back structure does not appear to determine the preference of *At*GRP7 for pri-miRNAs.

*At*GRP7 affects alternative splicing of pri-miR172b

*At*GRP7 overexpression leads to reduced levels of miR172b and miR172b* with a concomitant increase in pri-miR172b which contains introns both 5′ and 3′ of the stem–loop structure (Figure 6A). Because splicing of introns located 3′ of the stem–loop can impact accumulation of mature miRNAs (73,74), we asked whether *At*GRP7 affects splic-
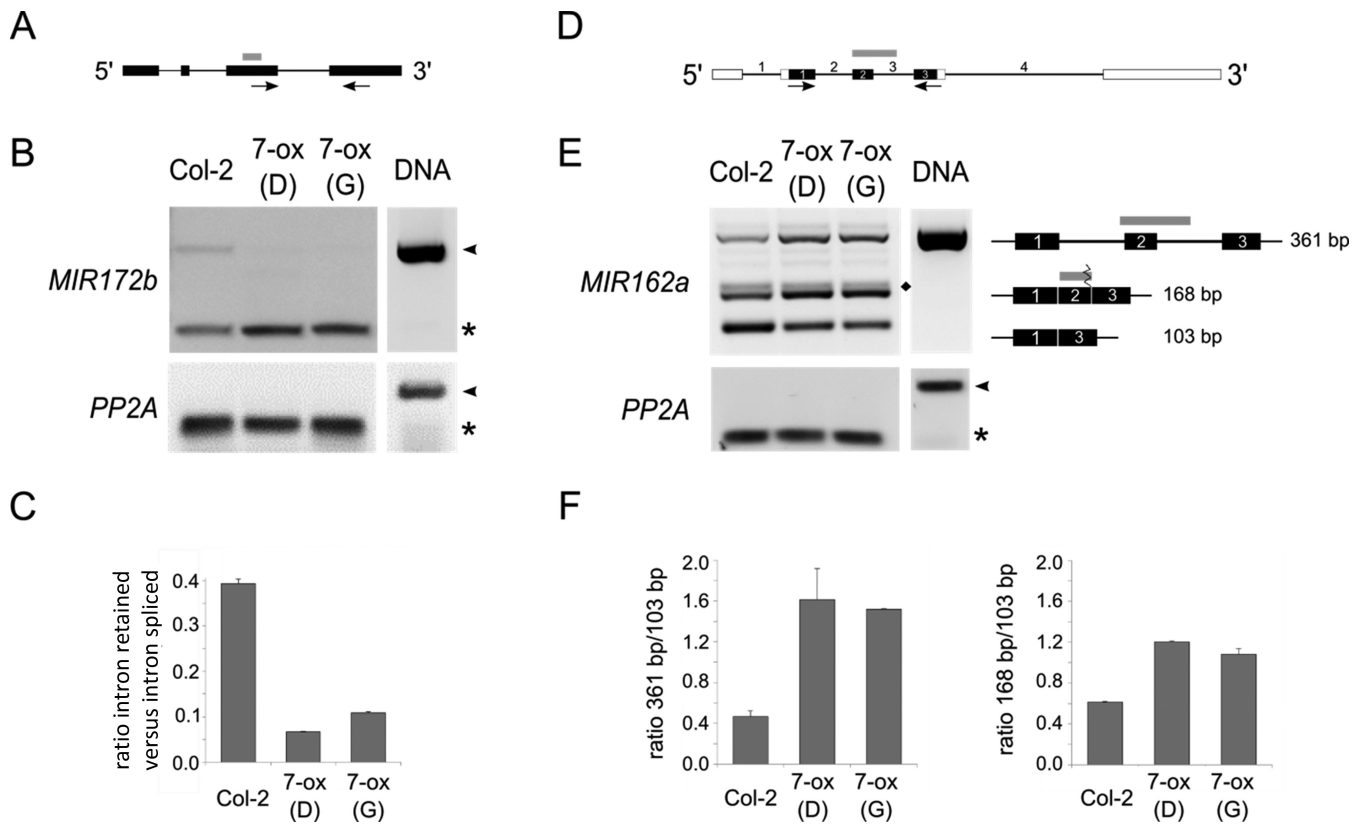
Figure 6. *At*GRP7 affects alternative splicing of pri-miRNAs. (**A**) Scheme of *MIR172b*. Black boxes = exons, grey box = position of the pri-miRNA, thin line = introns. The arrows denote the position of the primers used in (B). (**B**) RNA from the *At*GRP7-ox lines D and G and Col-2 wt was analysed by RT-PCR. The amplification products corresponding to the intron-retained form and the fully spliced forms are indicated by arrowheads and asterisks, respectively. *PP2A* served as a control. DNA = genomic DNA. (**C**) The ratio of intron-retained versus spliced pri-miR172b was quantified using Bioanalyzer DNA1000 chips. Shown is the mean of two reps. (**D**) Scheme of the non-protein-coding RNA harbouring *MIR162a*. Black boxes = exons, grey box = position of the pri-miRNA, open boxes = annotated 5′and 3′UTRs, thin line = introns. The arrows denote the position of the primers used in (E). (**E**) RNA from the *At*GRP7-ox lines D and G and Col-2 wt was analysed by RT-PCR. The transcript forms corresponding to the amplification products are indicated. The rhombus denotes an alternative version of the 168 nt band generated by an alternative 3′splice site 3 nt downstream of the authentic 3′splice site. *PP2A* served as a control. DNA = genomic DNA. (**F**) The ratio of the alternative splice forms versus the spliced form was quantified using Bioanalyzer DNA1000 chips. Shown is the mean of two reps.

ing of pri-miR172b. In wt plants, some pri-miR172b retaining the intron was detected in addition to the spliced form. In *At*GRP7-ox plants, the spliced pri-miR172b accumulated at the expense of the intron retained form, indicating that *At*GRP7 indeed affects splicing of pri-miRNAs (Figure 6B and C). In contrast, splicing of the introns located upstream of the hairpin was not altered (not shown). Thus, an enhanced assembly of the spliceosome at the 5′end of the downstream intron in *At*GRP7-ox plants may interfere with pri-miRNA processing. Alternatively, a slower release of miR172b and miR172b* caused by *At*GRP7 binding may allow more efficient assembly of the spliceosome.

While in animals around 80% of all miRNAs are encoded in introns, in Arabidopsis fewer miRNA genes are intronic (75). Among those is pri-miR162a located within an alternative intron of non-protein-coding RNA 78 (Figure 6D) (76). In *At*GRP7-ox plants, the unspliced precursor that retains the *MIR162a* gene is present at higher levels than in wt plants, whereas the isoform with exon 2 skipped that lacks the entire *MIR162a* gene is present at somewhat reduced levels (Figure 6E and F). An alternative isoform that retains exon 2 but lacks part of the stem–loop is present at

higher levels in *At*GRP7-ox plants. Thus, *At*GRP7 can also impact alternative splicing of an intronic pri-miRNA, but the level of mature miR162a was not significantly altered in *At*GRP7-ox plants. MiR162a targets *DCL1*, pointing to a complex feedback regulation between the miRNA and its target.

DISCUSSION

Here we show that the hnRNP-like protein *At*GRP7 affects steady-state abundance of a suite of miRNAs in Arabidopsis. Small RNA profiling of plants ectopically expressing *At*GRP7 identified subsets of miRNAs that accumulated either to lower or higher levels than in wt. Because most miRNAs with elevated levels showed only a low read coverage, we focussed on miRNAs with reduced levels.

One affected miRNA was miR398, and reduced miR398 levels correlated with increased levels of the miR398 targets CSD1, CSD2 and the copper chaperone CCS in *At*GRP7-ox plants. Importantly, the effect of *At*GRP7 on these miR398 targets was dependent on miR398, as upon deple-

tion of miR398 by high Cu^{2+} concentrations CSD and CCS levels in *At*GRP7-ox plants were indistinguishable from wt.

For a suite of miRNAs with reduced levels in *At*GRP7-ox plants, a reciprocal increase in pri-miRNA levels was observed in independent *At*GRP7-ox lines, implicating *At*GRP7 in processing of a number of pri-miRNAs into mature miRNAs. To test whether *At*GRP7 was required for pri-miRNA processing, we monitored miRNA and pri-miRNA levels in lines lacking *At*GRP7. In the *atgrp7–1* mutant, the levels of the tested miRNAs and pri-miRNAs were virtually unaltered relative to wt plants. This line lacks *At*GRP7 but has elevated levels of the paralogous protein *At*GRP8 due to relief from repression by *At*GRP7. Also in the *atgrp7–1 8i* line that lacks *At*GRP7 and expresses *At*GRP8 at wt levels due to an RNAi construct most tested miRNAs and pri-miRNAs remained at wt levels. Only for pri-miR398a and b were levels significantly reduced relative to wt and thus changed in opposite directions upon loss-of-function and *At*GRP7 overexpression, respectively, as predicted for a direct target.

This limited phenotype in the loss-of-function lines indicates that *At*GRP7 is not essential for the regulation of pri-miRNA processing. Thus, the impact of *At*GRP7 on miRNA metabolism observed in the *At*GRP7-ox plants may be unrelated to its function in wt plants and rather be attributed to non-physiological *At*GRP7 levels. However, we consider this unlikely for three reasons. Firstly, the accumulation of pri-miRNAs at the expense of mature miRNAs and the reciprocal increase in the miRNA targets were observed upon overexpression of *At*GRP7 but not upon expression to the same high level of a mutant variant of *At*GRP7 with a single amino acid exchange (*At*GRP7-R[49]Q) (Figure 2D). This is a strong hint that the impact of *At*GRP7 on miRNA metabolism is not an artefact of high protein levels but rather a specific function of the protein requiring its RNA-binding activity. The importance of R[49] for *At*GRP7 function has been demonstrated before: during infection of Arabidopsis plants with *Pseudomonas syringae*, R[49] is ADP-ribosylated by the bacterial effector HopU1 (36,77), interfering with *At*GRP7 binding to defense-related transcripts as part of the bacterial virulence strategy (29,39). Furthermore, the increased sensitivity of *atgrp7–1* to virulent *P. syringae* is complemented by a 3 kb genomic *AtGRP7* fragment but not the same fragment with R[49] mutated (29). Secondly, *in vivo* binding of *At*GRP7 to miRNA precursors supports our hypothesis that increased accumulation of several pri-miRNAs in *At*GRP7-ox plants is due to impaired processing. Importantly, the *At-GRP7::AtGRP7:*GFP *atgrp7–1* line used for RIP expresses *At*GRP7:GFP under control of the native promoter and noncoding regions in the absence of endogenous *At*GRP7 and thus has wt levels of *At*GRP7, ruling out any effect due to overexpression compared to wt levels. *In vivo* binding was observed for precursors of miRNAs with reduced levels in *At*GRP7-ox plants but not for those of miRNAs expressed at wt levels. Moreover, the pri-miRNAs were not enriched in immunoprecipitates from *AtGRP7::AtGRP7-R[49]Q:*GFP plants. This indicates that direct binding of the pri-miRNAs has functional significance for the impact of *At*GRP7 on pri-miRNA processing. Thirdly, in a previous microarray

analysis only 0.4% of the transcripts present on the ATH1 microarray changed >1.5-fold in *At*GRP7-ox lines relative to wt, arguing against a nonspecific misregulation of a large body of genes in *At*GRP7-ox plants (47).

Based on these observations, we rationalized that the limited miRNA phenotype of the *atgrp7* mutant lines may be due to redundancy with other regulatory proteins, an obvious candidate being the paralogous *At*GRP8 protein. In the absence of a true *atgrp8* loss-of-function line, we monitored the levels of several miRNA and pri-miRNAs that are regulated by *At*GRP7 in *At*GRP8-ox plants. Indeed, several pri-miRNAs accumulated at the expense of the mature miRNAs in the *At*GRP8-ox plants. Moreover, an *At*GRP8:GFP fusion protein expressed under control of the native promoter and the noncoding regions showed *in vivo* binding to the precursors of these miRNAs. Thus, we conclude that *At*GRP7 and *At*GRP8 inhibit processing of a suite of pri-miRNAs by direct binding, and that a lack of *At*GRP7 does not promote processing of these pri-miRNAs due to redundancy with *At*GRP8 and, perhaps, other regulatory proteins that remain to be identified.

In line with a direct role in pri-miRNA processing, *At*GRP7 colocalizes with DCL1, HYL1, CBP80 and SE in the nucleus. Furthermore, steady-state levels of components known to be involved in miRNA biogenesis were not altered in *At*GRP7-ox plants, consistent with a previous microarray analysis (47) and arguing against an indirect effect. Several RBPs with different types of RNA-binding domains have been shown to co-operate with DCL1, including HYL1 with a double-stranded RNA-binding domain (22,78,79), SE with a zinc finger (19,80), TOUGH with a G patch domain (18) and the CAP binding complex (CBC) subunits CBP20 and CBP80 (19,20). These proteins have a more global impact on pri-miRNA processing whereas *At*GRP7 affects processing of a limited set of pri-miRNAs. Furthermore, these DCL1-interacting proteins promote processing whereas *At*GRP7 appears to mostly act as an inhibitor.

*At*GRP7 is the first plant hnRNP-like protein shown to regulate miRNA biogenesis. A role for an hnRNP in the processing of a miRNA has first been described for human hnRNP A1 (81). HnRNP A1 binds specifically to pri-miR-18a and the resulting conformational change likely facilitates its processing (82). Notably, hnRNP A1 can also act as an inhibitor of miRNA biogenesis: hnRNP A1 binding to the terminal loop of pri-let-7a interferes with binding of KSPR that promotes pri-let-7a processing (83,84). For *At*GRP7, the inhibition of pri-miRNA processing appears to involve direct *in vivo* binding to the pri-miRNAs. Thus, the reduced processing of these pri-miRNAs may be caused by steric hindrance of an activator or by conformational changes. In contrast, the effect of *At*GRP7 on miRNAs with elevated levels may be indirect, as the corresponding pri-miRNA levels were not reduced in *At*GRP7-ox plants and the pri-miRNAs were not enriched in RIP assays.

To begin to understand the molecular basis of *At*GRP7 action, we searched for common properties of the pri-miRNAs that are controlled by *At*GRP7. In contrast to mammalian pri-miRNAs, plant miRNA precursors display stem–loops of highly variable size that may pose additional challenges to the processing machinery (72). Comparison of the length of the stem–loop of pri-miRNAs annotated in

miRBase with the size distribution of precursors with significantly altered levels in *At*GRP7-ox plants revealed no difference. Processing of the pri-miRNAs mostly involves an initial cleavage at the base of the stem and proceeds to the loop. Recently, several pri-miRNAs have been shown to be processed with the first cut at the loop, proceeding to the base (64). Moreover, depending on the number of cuts by DCL1 to release the mature miRNA, sequential base-to-loop and sequential loop-to-base mechanisms have been defined if more than one cut by DCL1 is required to release the mature miRNA (72). Among the pri-miRNAs binding to *At*GRP7 *in vivo* was pri-miR159a which is processed via an initial cut at the loop (64). Thus, *At*GRP7 appears to affect miRNA precursors processed by the conventional base-to-loop mechanism or in loop-to-base direction. Moreover, among the differentially expressed miRNAs are several that are generated by sequential cuts (indicated in Supplementary Tables S4 and S5).

Altered levels of miRNAs in *At*GRP7-ox plants may also be due to imprecise processing of pri-miRNAs such that the excised miRNAs would not fall exactly within the annotated mature miRNA. However, the processing accuracy was not altered upon *At*GRP7 overexpression, different from what has been observed in *hyl1* and *se* mutants (85). In the future, the establishment of crosslinking and immunoprecipitation techniques in plants to determine *in vivo* binding sites will help to define pri-miRNA features recognized by *At*GRP7.

Recently, a reciprocal interaction between splicing of introns in pri-miRNAs that are located downstream of the stem–loop and accumulation of the corresponding mature miRNA has been described (73,74). We find that splicing of the pri-miR172b intron located downstream of the stem–loop is favored in *At*GRP7-ox plants compared to wt with concomitantly reduced levels of miR172b and miR172b*. Because *At*GRP7 affects alternative splicing of pre-mRNAs, it may promote removal of the intron and lead to reduced miR172b levels. On the other hand, impaired processing of the stem–loop may allow more efficient splicing of the intron, as observed for *dcl1* mutants (73). However, the role of *At*GRP7 in inhibiting processing is not contingent on removal of introns, as it also affects steady-state levels of miRNAs derived from intron-less pri-miRNAs, e.g. pri-miR167a and pri-miR172e. In turn, *At*GRP7 affects alternative splicing of pri-miR162a (30) but the level of mature miR162a is not significantly altered in *At*GRP7-ox plants. Thus, the common features of pri-miRNAs regulated by *At*GRP7 remain to be determined.

Taken together, *At*GRP7 is the first hnRNP-like protein in plants with a dual role in alternative splicing of pre-mRNAs and maturation of pri-miRNAs. This resembles the function of SE and the CBC (19,86). For *At*GRP7, regulation of some of its splicing substrates is due to direct binding *in vivo*, not yet shown for SE or the CBC (30). *At*GRP7 not only directly impacts mRNAs through alternative splicing but also indirectly via pri-miRNA processing and consequently miRNA levels, supporting the view of extensive cross-talk between regulation by RBPs and miRNAs.

REFERENCES

1. Staiger,D. (2001) RNA-binding proteins and circadian rhythms in *Arabidopsis thaliana*. *Philos. Trans. R. Soc. Lond. B Biol. Sci.*, **356**, 1755–1759.
2. Terzi,L.C. and Simpson,G.G. (2008) Regulation of flowering time by RNA processing. *Curr. Top. Microbiol. Immunol.*, **326**, 201–218.
3. Lorkovic,Z.J. (2009) Role of plant RNA-binding proteins in development, stress response and genome organization. *Trends Plant Sci.*, **14**, 229–236.
4. Smith,C.W.J. and Valcarel,J. (2000) Alternative pre-mRNA splicing: the logic of combinatorial control. *Trends Biochem. Sci.*, **25**, 381–388.
5. Wachter,A., Rühl,C. and Stauffer,E. (2012) The role of polypyrimidine tract-binding proteins and other hnRNP proteins in plant splicing regulation. *Front. Plant Sci.*, **3**, 81.
6. Han,S.P., Tang,Y.H. and Smith,R. (2010) Functional diversity of the hnRNPs: past, present and perspectives. *Biochem. J.*, **430**, 379–392.
7. Rubio-Somoza,I. and Weigel,D. (2011) MicroRNA networks and developmental plasticity in plants. *Trends Plant Sci.*, **16**, 258–264.
8. Voinnet,O. (2009) Origin, biogenesis, and activity of plant microRNAs. *Cell*, **136**, 669–687.
9. Rogers,K. and Chen,X. (2013) Biogenesis, turnover, and mode of action of plant microRNAs. *Plant Cell* **25**, 2383–2399.
10. Xie,Z., Allen,E., Fahlgren,N., Calamar,A., Givan,S.A. and Carrington,J.C. (2005) Expression of Arabidopsis MIRNA genes. *Plant Physiol.*, **138**, 2145–2154.
11. Yu,B., Bi,L., Zheng,B., Ji,L., Chevalier,D., Agarwal,M., Ramachandran,V., Li,W., Lagrange,T., Walker,J.C. *et al.* (2008) The FHA domain proteins DAWDLE in Arabidopsis and SNIP1 in humans act in small RNA biogenesis. *Proc. Natl Acad. Sci. U.S.A.*, **105**, 10073–10078.
12. Yu,B., Yang,Z., Li,J., Minakhina,S., Yang,M., Padgett,R.W., Steward,R. and Chen,X. (2005) Methylation as a crucial step in plant microRNA biogenesis. *Science*, **307**, 932–935.
13. Yang,Z., Ebright,Y.W., Yu,B. and Chen,X. (2006) HEN1 recognizes 21–24 nt small RNA duplexes and deposits a methyl group onto the 2′ OH of the 3′ terminal nucleotide. *Nucleic Acids Res.* **34**, 667–675.
14. Brodersen,P., Sakvarelidze-Achard,L., Bruun-Rasmussen,M., Dunoyer,P., Yamamoto,Y.Y., Sieburth,L. and Voinnet,O. (2008) Widespread translational inhibition by plant miRNAs and siRNAs. *Science*, **320**, 1185–1190.
15. Schwab,R., Palatnik,J.F., Riester,M., Schommer,C., Schmid,M. and Weigel,D. (2005) Specific effects of microRNAs on the plant transcriptome. *Dev. Cell*, **8**, 517–527.
16. Mi,S., Cai,T., Hu,Y., Chen,Y., Hodges,E., Ni,F., Wu,L., Li,S., Zhou,H., Long,C. *et al.* (2008) Sorting of small RNAs into Arabidopsis argonaute complexes is directed by the 5′ terminal nucleotide. *Cell*, **133**, 116–127.
17. Zhang,X., Zhao,H., Gao,S., Wang,W.C., Katiyar-Agarwal,S., Huang,H.D., Raikhel,N. and Jin,H. (2011) Arabidopsis Argonaute 2 regulates innate immunity via miRNA393-mediated silencing of a Golgi-localized SNARE gene, MEMB12. *Mol. Cell*, **42**, 356–366.

18. Ren,G., Xie,M., Dou,Y., Zhang,S., Zhang,C. and Yu,B. (2012) Regulation of miRNA abundance by RNA binding protein TOUGH in Arabidopsis. *Proc. Natl Acad. Sci. U.S.A.*, **109**, 12817–12821.

19. Laubinger,S., Sachsenberg,T., Zeller,G., Busch,W., Lohmann,J.U., Ratsch,G. and Weigel,D. (2008) Dual roles of the nuclear cap-binding complex and SERRATE in pre-mRNA splicing and microRNA processing in Arabidopsis thaliana. *Proc. Natl Acad. Sci. U.S.A.*, **105**, 8795–8800.

20. Kim,S., Yang,J.-Y., Xu,J., Jang,I.-C., Prigge,M.J. and Chua,N.-H. (2008) Two CAP BINDING PROTEINS CBP20 and CBP80 are involved in processing primary microRNAs. *Plant Cell Physiol.*, **49**, 1634–1644.

21. Gregory,B.D., O'Malley,R.C., Lister,R., Urich,M.A., Tonti-Filippini,J., Chen,H., Millar,A.H. and Ecker,J.R. (2008) A link between RNA metabolism and silencing affecting Arabidopsis development. *Dev. Cell*, **14**, 854–866.

22. Kurihara,Y., Takashi,Y. and Watanabe,Y. (2006) The interaction between DCL1 and HYL1 is important for efficient and precise processing of pri-miRNA in plant microRNA biogenesis. *RNA*, **12**, 206–212.

23. Manavella,Pablo A., Hagmann,J., Ott,F., Laubinger,S., Franz,M., Macek,B. and Weigel,D. (2012) Fast-forward genetics identifies plant CPL phosphatases as regulators of miRNA processing factor HYL1. *Cell*, **151**, 859–870.

24. Heintzen,C., Melzer,S., Fischer,R., Kappeler,S., Apel,K. and Staiger,D. (1994) A light- and temperature-entrained circadian clock controls expression of transcripts encoding nuclear proteins with homology to RNA-binding proteins in meristematic tissue. *Plant J.*, **5**, 799–813.

25. Carpenter,C.D., Kreps,J.A. and Simon,A.E. (1994) Genes encoding glycine-rich *Arabidopsis thaliana* proteins with RNA-binding motifs are influenced by cold treatment and an endogenous circadian rhythm. *Plant Physiol.*, **104**, 1015–1025.

26. Schmidt,F., Marnef,A., Cheung,M.-K., Wilson,I., Hancock,J., Staiger,D. and Ladomery,M. (2010) A proteomic analysis of oligo(dT)-bound mRNP containing oxidative stress-induced *Arabidopsis thaliana* RNA-binding proteins *AT*GRP7 and *AT*GRP8. *Mol. Biol. Rep.*, **37**, 839–845.

27. Kim,J.S., Jung,H.J., Lee,H.J., Kim,K.A., Goh,C.H., Woo,Y., Oh,S.H., Han,Y.S. and Kang,H. (2008) Glycine-rich RNA-binding protein7 affects abiotic stress responses by regulating stomata opening and closing in Arabidopsis thaliana. *Plant J.*, **55**, 455–466.

28. Schöning,J.C., Streitner,C., Meyer,I.M., Gao,Y. and Staiger,D. (2008) Reciprocal regulation of glycine-rich RNA-binding proteins via an interlocked feedback loop coupling alternative splicing to nonsense-mediated decay in Arabidopsis. *Nucleic Acids Res.*, **36**, 6977–6987.

29. Nicaise,V., Joe,A., Jeong,B., Korneli,C., Boutrot,F., Wested,I., Staiger,D., Alfano,J.R. and Zipfel,C. (2013) Pseudomonas HopU1 affects interaction of plant immune receptor mRNAs to the RNA-binding protein GRP7. *EMBO J.*, **32**, 701–712.

30. Streitner,C., Köster,T., Simpson,C.G., Shaw,P., Danisman,S., Brown,J.W.S. and Staiger,D. (2012) An hnRNP-like RNA-binding protein affects alternative splicing by in vivo interaction with target transcripts in Arabidopsis thaliana. *Nucleic Acids Res.*, **40**, 11240–11255.

31. Heintzen,C., Nater,M., Apel,K. and Staiger,D. (1997) *At*GRP7, a nuclear RNA-binding protein as a component of a circadian-regulated negative feedback loop in *Arabidopsis thaliana*. *Proc. Natl Acad. Sci. U.S.A.*, **94**, 8515–8520.

32. Schöning,J.C., Streitner,C., Page,D.R., Hennig,S., Uchida,K., Wolf,E., Furuya,M. and Staiger,D. (2007) Autoregulation of the circadian slave oscillator component *At*GRP7 and regulation of its targets is impaired by a single RNA recognition motif point mutation. *Plant J.*, **52**, 1119–1130.

33. Streitner,C., Danisman,S., Wehrle,F., Schöning,J.C., Alfano,J.R. and Staiger,D. (2008) The small glycine-rich RNA-binding protein *At*GRP7 promotes floral transition in *Arabidopsis thaliana*. *Plant J.*, **56**, 239–250.

34. Löhr,B., Streitner,C., Steffen,A., Lange,T. and Staiger,D. (2014) A glycine-rich RNA-binding protein affects gibberellin biosynthesis in Arabidopsis. *Mol. Biol. Rep.*, **41**, 439–445.

35. Staiger,D. and Apel,K. (1999) Circadian clock-regulated expression of an RNA-binding protein in Arabidopsis: characterisation of a minimal promoter element. *Mol. Gen. Genet.*, **261**, 811–819.

36. Fu,Z.Q., Guo,M., Jeong,B.R., Tian,F., Elthon,T.E., Cerny,R.L., Staiger,D. and Alfano,J.R. (2007) A type III effector ADP-ribosylates RNA-binding proteins and quells plant immunity. *Nature*, **447**, 284–288.

37. Staiger,D., Apel,K. and Trepp,G. (1999) The Atger3 promoter confers circadian clock-regulated transcription with peak expression at the beginning of the night. *Plant Mol. Biol. Rep.*, **40**, 873–882.

38. Pall,G.S. and Hamilton,A.J. (2008) Improved northern blot method for enhanced detection of small RNA. *Nat. Protoc.*, **3**, 1077–1084.

39. Hackmann,C., Korneli,C., Kutyniok,M., Köster,T., Wiedenlübbert,M., Müller,C. and Staiger,D. (2014) Salicylic acid-dependent and -independent impact of an RNA-binding protein on plant immunity. *Plant Cell Environ.*, **37**, 696–706.

40. Speth,C., Willing,E.-M., Rausch,S., Schneeberger,K. and Laubinger,S. (2013) RACK1 scaffold proteins influence miRNA abundance in Arabidopsis. *Plant J.*, **76**, 433–445.

41. Köster,T. and Staiger,D. (2014) RNA-binding protein immunoprecipitation from whole-cell extracts. *Methods in Molecular Biology*, **1062**, 679–695.

42. Langmead,B., Trapnell,C., Pop,M. and Salzberg,S.L. (2009) Ultrafast and memory-efficient alignment of short DNA sequences to the human genome. *Genome Biol.*, **10**, R25.

43. Quinlan,A.R. and Hall,I.M. (2010) BEDTools: a flexible suite of utilities for comparing genomic features. *Bioinformatics*, **26**, 841–842.

44. Anders,S. and Huber,W. (2010) Differential expression analysis for sequence count data. *Genome Biol.*, **11**, R106.

45. Heintzen,C., Fischer,R., Melzer,S., Kappeler,S., Apel,K. and Staiger,D. (1994) Circadian oscillations of a transcript encoding a germin-like protein that is associated with cell walls in young leaves of the long-day plant Sinapis alba L. *Plant Physiol.*, **106**, 905–915.

46. Lummer,M., Humpert,F., Steuwe,C., Schüttpelz,M., Sauer,M. and Staiger,D. (2011) Reversible photoswitchable DRONPA-s monitors nucleocytoplasmic transport of an RNA-binding protein in transgenic plants. *Traffic*, **12**, 693–702.

47. Streitner,C., Hennig,L., Korneli,C. and Staiger,D. (2010) Global transcript profiling of transgenic plants constitutively overexpressing the RNA-binding protein AtGRP7. *BMC Plant Biol.*, **10**, 221.

48. Bonnet,E., Wuyts,J., Rouze,P. and Van de Peer,Y. (2004) Detection of 91 potential conserved plant microRNAs in Arabidopsis thaliana and Oryza sativa identifies important target genes. *Proc. Natl Acad. Sci. U.S.A.*, **101**, 11511–11516.

49. Jones-Rhoades,M.W. and Bartel,D.P. (2004) Computational identification of plant microRNAs and their targets, including a stress-induced miRNA. *Mol. Cell*, **14**, 787–799.

50. Beauclair,L., Yu,A. and Bouche,N. (2010) MicroRNA-directed cleavage and translational repression of the copper chaperone for superoxide dismutase mRNA in Arabidopsis. *Plant J.*, **62**, 454–462.

51. Dugas,D.V. and Bartel,B. (2008) Sucrose induction of Arabidopsis miR398 represses two Cu/Zn superoxide dismutases. *Plant Mol. Biol.*, **67**, 403–417.

52. Sunkar,R., Kapoor,A. and Zhu,J.K. (2006) Posttranscriptional induction of Two Cu/Zn superoxide dismutase genes in Arabidopsis is mediated by downregulation of miR398 and important for oxidative stress tolerance. *Plant Cell*, **18**, 2051–2065.

53. Yamasaki,H., Abdel-Ghany,S.E., Cohu,C.M., Kobayashi,Y., Shikanai,T. and Pilon,M. (2007) Regulation of copper homeostasis by micro-RNA in Arabidopsis. *Biol. Chem.*, **282**, 16369–16378.

54. Yamaguchi,A., Wu,M.F., Yang,L., Wu,G., Poethig,R.S. and Wagner,D. (2009) The microRNA-regulated SBP-Box transcription factor SPL3 is a direct upstream activator of LEAFY, FRUITFULL, and APETALA1. *Dev. Cell*, **17**, 268–278.

55. Allen,E., Xie,Z., Gustafson,A.M. and Carrington,J.C. (2005) microRNA-directed phasing during trans-acting siRNA biogenesis in plants. *Cell*, **121**, 207–221.

56. Chen,X. (2004) A microRNA as a translational repressor of APETALA2 in Arabidopsis flower development. *Science*, **303**, 2022–2025.

57. Mathieu,J., Yant,L.J., Murdter,F., Kuttner,F. and Schmid,M. (2009) Repression of flowering by the miR172 target SMZ. *PLoS Biol.*, **7**, e1000148.

58. Rhoades,M.W., Reinhart,B.J., Lim,L.P., Burge,C.B., Bartel,B. and Bartel,D.P. (2002) Prediction of plant microRNA targets. *Cell*, **110**, 513–520.

59. Cuperus,J.T., Fahlgren,N. and Carrington,J.C. (2011) Evolution and functional diversification of MIRNA genes. *Plant Cell* **23**, 431–442.

60. de Meaux,J., Hu,J.-Y., Tartler,U. and Goebel,U. (2008) Structurally different alleles of the ath-MIR824 microRNA precursor are maintained at high frequency in Arabidopsis thaliana. *Proc. Natl Acad. Sci. U.S.A.*, **105**, 8994–8999.

61. Kutter,C., Schob,H., Stadler,M., Meins,F. Jr and Si-Ammour,A. (2007) MicroRNA-mediated regulation of stomatal development in Arabidopsis. *Plant Cell*, **19**, 2417–2429.

62. Allen,R.S., Li,J., Stahle,M.I., Dubroue,A., Gubler,F. and Millar,A.A. (2007) Genetic analysis reveals functional redundancy and the major target genes of the Arabidopsis miR159 family. *Proc. Natl Acad. Sci. U.S.A.*, **104**, 16371–16376.

63. Zhang,W., Gao,S., Zhou,X., Chellappan,P., Chen,Z., Zhou,X., Zhang,X., Fromuth,N., Coutino,G., Coffey,M. *et al.* (2011) Bacteria-responsive microRNAs regulate plant innate immunity by modulating plant hormone networks. *Plant Mol. Biol.*, **75**, 93–105.

64. Bologna,N.G., Mateos,J.L., Bresso,E.G. and Palatnik,J.F. (2009) A loop-to-base processing mechanism underlies the biogenesis of plant microRNAs miR319 and miR159. *EMBO J.*, **28**, 3646–3656.

65. Wu,X., Shi,Y., Li,J., Xu,L., Fang,Y., Li,X. and Qi,Y. (2013) A role for the RNA-binding protein MOS2 in microRNA maturation in Arabidopsis. *Cell Res.*, **23**, 645–657.

66. Zhan,X., Wang,B., Li,H., Liu,R., Kalia,R.K., Zhu,J.-K. and Chinnusamy,V. (2013) Arabidopsis proline-rich protein important for development and abiotic stress tolerance is involved in microRNA biogenesis. *Proc. Natl Acad. Sci. U.S.A.*, **109**, 18198–18203.

67. Zhang,S., Xie,M., Ren,G. and Yu,B. (2013) CDC5, a DNA binding protein, positively regulates posttranscriptional processing and/or transcription of primary microRNA transcripts. *Proc. Natl Acad. Sci. U.S.A.*, **110**, 17588–17593.

68. Rajagopalan,R., Vaucheret,H., Trejo,J. and Bartel,D.P. (2006) A diverse and evolutionarily fluid set of microRNAs in *Arabidopsis thaliana. Genes Dev.*, **20**, 3407–3425.

69. Fang,Y. and Spector,D.L. (2007) Identification of nuclear dicing bodies containing proteins for microRNA biogenesis in living Arabidopsis plants. *Curr. Biol.*, **17**, 818–823.

70. Song,L., Han,M.H., Lesicka,J. and Fedoroff,N. (2007) Arabidopsis primary microRNA processing proteins HYL1 and DCL1 define a nuclear body distinct from the Cajal body. *Proc. Natl Acad. Sci. U.S.A.*, **104**, 5437–5442.

71. Fujioka,Y., Utsumi,M., Ohba,Y. and Watanabe,Y. (2007) Location of a possible miRNA processing site in SmD3/SmB nuclear bodies in Arabidopsis. *Plant Cell Physiol.*, **48**, 1243–1253.

72. Bologna,N.G., Schapire,A.L., Zhai,J., Chorostecki,U., Boisbouvier,J., Meyers,B.C. and Palatnik,J.F. (2013) Multiple RNA recognition patterns during microRNA biogenesis in plants. *Genome Res.*, **23**, 1675–1689.

73. Schwab,R., Speth,C., Laubinger,S. and Voinnet,O. (2013) Enhanced microRNA accumulation through stemloop-adjacent introns. *EMBO Rep.*, **14**, 615–621.

74. Bielewicz,D., Kalak,M., Kalyna,M., Windels,D., Barta,A., Vazquez,F., Szweykowska-Kulinska,Z. and Jarmolowski,A. (2013) Introns of plant pri-miRNAs enhance miRNA biogenesis. *EMBO Rep.*, **14**, 622–628.

75. Brown,J.W.S., Marshall,D.F. and Echeverria,M. (2008) Intronic noncoding RNAs and splicing. *Trends Plant Sci.*, **13**, 335–342.

76. Hirsch,J., Lefort,V., Vankersschaver,M., Boualem,A., Lucas,A., Thermes,C., d'Aubenton-Carafa,Y. and Crespi,M. (2006) Characterization of 43 non-protein-coding mRNA genes in Arabidopsis, including the MIR162a-derived transcripts. *Plant Physiol.*, **140**, 1192–1204.

77. Jeong,B.-r., Lin,Y., Joe,A., Guo,M., Korneli,C., Yang,H., Wang,P., Yu,M., Cerny,R.L., Staiger,D. *et al.* (2011) Structure function analysis of an ADP-ribosyltransferase type III effector and its RNA-binding target in plant immunity. *J. Biol. Chem.*, **286**, 43272–43281.

78. Han,M.-H., Goud,S., Song,L. and Fedoroff,N. (2004) The Arabidopsis double-stranded RNA-binding protein HYL1 plays a role in microRNA-mediated gene regulation. *Proc. Natl Acad. Sci. U.S.A.*, **101**, 1093–1098.

79. Vazquez,F., Gasciolli,V., Crete,P. and Vaucheret,H. (2004) The nuclear dsRNA binding protein HYL1 is required for microRNA accumulation and plant development, but not posttranscriptional transgene silencing. *Curr. Biol.*, **14**, 346–351.

80. Iwata,Y., Takahashi,M., Fedoroff,N.V. and Hamdan,S.M. (2013) Dissecting the interactions of SERRATE with RNA and DICER-LIKE 1 in Arabidopsis microRNA precursor processing. *Nucleic Acids Res.*, **41**, 9129–9140.

81. Guil,S. and Caceres,J.F. (2007) The multifunctional RNA-binding protein hnRNP A1 is required for processing of miR-18a. *Nat. Struct. Mol. Biol.*, **14**, 591–596.

82. Michlewski,G., Guil,S., Semple,C.A. and Caceres,J.F. (2008) Posttranscriptional regulation of miRNAs harboring conserved terminal loops. *Mol. Cell*, **32**, 383–393.

83. Michlewski,G. and Caceres,J.F. (2010) Antagonistic role of hnRNP A1 and KSRP in the regulation of let-7a biogenesis. *Nat. Struct. Mol. Biol.*, **17**, 1011–1018.

84. Trabucchi,M., Briata,P., Garcia-Mayoral,M., Haase,A.D., Filipowicz,W., Ramos,A., Gherzi,R. and Rosenfeld,M.G. (2009) The RNA-binding protein KSRP promotes the biogenesis of a subset of microRNAs. *Nature*, **459**, 1010–1014.

85. Dong,Z., Han,M.H. and Fedoroff,N. (2008) The RNA-binding proteins HYL1 and SE promote accurate in vitro processing of pri-miRNA by DCL1. *Proc. Natl Acad. Sci. U.S.A.*, **105**, 9970–9975.

86. Raczynska,K.D., Stepien,A., Kierzkowski,D., Kalak,M., Bajczyk,M., McNicol,J., Simpson,C.G., Szweykowska-Kulinska,Z., Brown,J.W.S. and Jarmolowski,A. (2013) The SERRATE protein is involved in alternative splicing in Arabidopsis thaliana. *Nucleic Acids Res.*, **42**, 1224–1244.